Conductance Quantization in Gold Nanowires

Curran D. Muhlberger

Department of Physics, Cornell University, Ithaca, New York 14853

(Dated: April 10, 2009)

Using a piezoelectric transducer to repeatedly create and break contact between two gold wires, we measure the conductance of nanowires formed just prior to separation. The histogram of these conductances exhibits a clear peak at $G_0 = 2e^2/h$, the fundamental quantum of conductance, and two smaller peaks near integer multiples of this value. Our measurement of $G_0 = (7.77 \pm 0.14) \times 10^{-5}\,\mathrm{S}$ lies within 0.3% of the theoretical value, and the first and second conductance peaks lie in a ratio of 2.000 ± 0.050, consistent with integral quantization. In performing this analysis, we identified differential nonlinearities in our digital oscilloscope corresponding to a 10% spread in bin sizes and successfully compensated for their effects using histograms of voltage ramps.

I. INTRODUCTION

In macroscopic metallic wires, electrical resistance arises as electrons scatter off of impurities in the metal. However, at the nanoscale, the length of the wire may be shorter than the mean free path of electrons, resulting in ballistic transport. If the width of these wires is also reduced to a size comparable to the Fermi wavelength of the electrons, the wave nature of the electrons can no longer be neglected. Such systems are called quantum point contacts (QPCs) (Hansen *et al.*, 1997), and their behavior has important implications for miniaturized communications equipment and other nanotechnologies (Costa-Krämer *et al.*, 1995).

In the past two decades, researchers have used a variety of techniques to create and study QPCs. These include two-dimensional electron gasses in GaAs-AlGaAs heterojunctions, scanning tunneling microscope tips driven into metals, mechanically controllable break junctions, and metallic wires brought into contact and separated (Hansen *et al.*, 1997; van Houten and Beenakker, 1996). The last of these techniques yields short-lived QPCs in the form of metallic nanowires as the two samples prepare to separate. In particular, gold wires are appealing candidates, as gold's inertness resists contamination of the contact surfaces in an open-air environment, eliminating the need for the ultra-high vacuum required by other methods.

Theory suggests that nanowires formed in this way should each possess a resistance of $R_0 = 12.9\,\mathrm{k\Omega}$, which is a highly macroscopic quantity arising from a quantum-mechanical effect. Equivalently, the conductance of these wires should be quantized in units of $G_0 = 2e^2/h$. Here we present a relatively simple method for observing this quantization and performing precision measurements on it using a statistical analysis of many automated trials. Aside from testing the theory of QPCs and characterizing the behavior of gold nanowires in particular, our procedure demonstrates the effects of quantum mechanics in a clear way with a minimum of specialized equipment.

II. THEORY

The conductance G of a quantum point contact is expected to obey the Landauer formula

$$G = \frac{2e^2}{h}\,\mathrm{tr}(TT^\dagger) = \frac{2e^2}{h}\sum_n t_n\,, \tag{1}$$

where e is the elementary charge, h is Planck's constant, and T is the transmission matrix for electrons traversing the contact. The prefactor of 2 reflects the twofold degeneracy in electron spin (intermediate conductances being possible with the application of a magnetic field) (Khurana, 1988). By diagonalizing T in a basis of non-mixing eigenchannels, the eigenvalues t_n of $TT^\dagger$ simply represent the transmission probabilities of each of the channels (Hansen *et al.*, 1997). For ideal ballistic transport in N eigenmodes, exactly N of these probabilities are equal to 1 while the others vanish, yielding an overall conductance of $G = 2Ne^2/h$ (van Houten and Beenakker, 1996).

Considering the case of a single, ideal transmission channel, Eq. 1 suggests that the fundamental quantum of conductance should be equal to

$$G_0 = \frac{2e^2}{h} = 77.5\,\mu\mathrm{S} = \frac{1}{12.9\,\mathrm{k\Omega}}\,. \tag{2}$$

Conductance for ballistic systems with multiple channels, such as collections of N nanowires, will thus be quantized in integer multiples of G_0. One model for understanding this quantization is to treat the contact as a waveguide for the electrons in the current, noting that for contacts whose width is comparable to the Fermi wavelength, the quantum-mechanical wave nature of the electrons cannot be neglected. In a waveguide, each propagating mode has a characteristic cutoff frequency that must be exceeded before transmission will take place (Khurana, 1988). Therefore, the conductance of the contact will increase in equal steps for each new transmission channel made available, either by changing the contact geometry or by establishing additional contacts. The fact that the resistance of these channels is non-zero is due

to reflections between these eigenmodes and the propagating modes in the leads (van Houten and Beenakker, 1996).

Metalic nanowires are a particularly convenient type of quantum point contact, as the Fermi wavelength in metals is comparable to atomic separations and thus to the width of wires composed of chains of atoms (van Houten and Beenakker, 1996). They can be created when two samples of metal are brought into contact and then separated again, forming just before the contact is severed (Costa-Krämer *et al.*, 1995). The original junction between the two samples need not be microscopic.

Rodrigues et al. have observed three possible atomic arrangements for gold nanowires and attribute a different set of available conductances to each one (Rodrigues *et al.*, 2000). Considering plots of conductance versus time as a nanowire is severed, they conclude that plateaus at $1G_0$ would be expected in $7/13$ of breaking cases and that only $4/7$ of those would also exhibit a plateau at $2G_0$. The arrangements associated with the remaining $6/13$ of cases allow for a plateau at $2G_0$ that decays directly to 0. Comparisons with these expected ratios is beyond the scope of this study, though it presents itself as a natural extension of our methods.

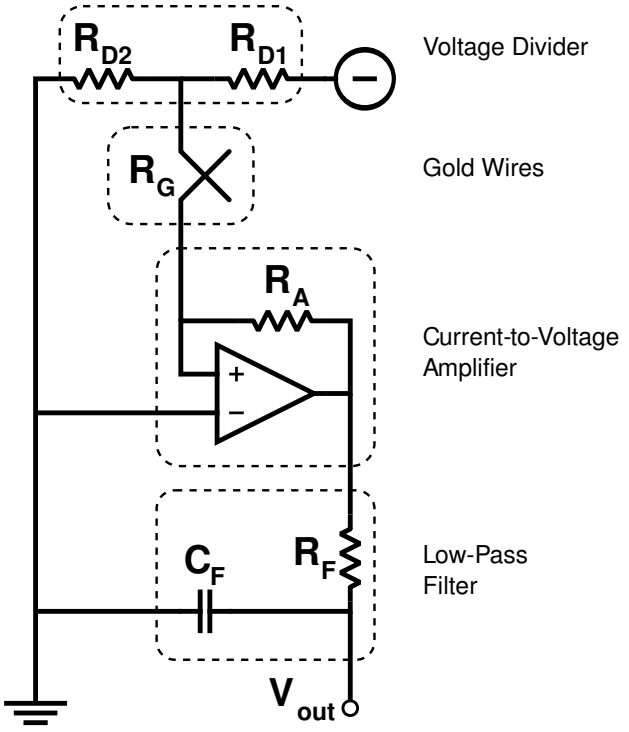

Figure 1 Schematic for the current-to-voltage amplifier circuit.

III. EXPERIMENTAL SETUP

In order to measure the value of the fundamental unit conductance and to determine whether or not nanowire conductance is indeed quantized, we designed a system to acquire oscilloscope traces of voltage drops across a junction of gold wires as that junction was repeatedly broken. With sufficiently many traces, we could construct a histogram of voltages whose peaks, if prominent and evenly spaced, would correspond to multiples of the fundamental quantum of conductance.

We employed a digital sampling oscilloscope (DSO) to acquire snapshots of voltage versus time in digital form. Our particular model was an 8-bit Link Instruments DSO-8502 capable of recording at 500 MHz. A piezoelectric transducer from RadioShack, designed to resonate at 2500 Hz, was used as an actuator and driven by a Wavetek Model 180 sweep/function generator. For measuring and calibrating various circuit components, we relied on a Micronta 22-185 digital multimeter.

The first phase of our experiment attempted to duplicate the results of Costa-Krämer et al. by visually examining oscilloscope traces as a junction was broken by mechanical vibrations (Costa-Krämer *et al.*, 1995). This junction was created by attaching gold wires to the tips of long, relatively stiff copper leads and positioning the leads so that one tip very lightly rested on top of the other. Vibrating the experimental setup, such as by tapping on the lab bench, caused these tips to oscillate at the ends of their lever arms with a relatively slow frequency. These small oscillations brought the tips in and out of contact, breaking and reforming the junction and stringing out nanowires in the process.

The conductance (or resistance) of this junction can be measured using a current-to-voltage amplifier circuit, such as that shown in Fig. 1. A voltage divider reduces the rail voltage by more than two orders of magnitude in order to protect the circuit when the junction is closed. An LT1007 operational amplifier and feedback resistor allow the current flowing through the junction to be measured by a proportional voltage. The low-pass filter greatly reduces noise in the output signal at the expense of minor smoothing of sharp features (such as abrupt nanowire severage).

The resistances used in the voltage divider were $R_{D1} = (21.72 \pm 0.01)\,\mathrm{k\Omega}$ and $R_{D2} = (51.2 \pm 0.1)\,\Omega$, providing the gold wire junction with $(23.57 \pm 0.05)\,\mathrm{mV}$ given $\pm 10\,\mathrm{V}$ rails. The amplifer gain was provided by a resistance of $R_A = (85.90 \pm 0.05)\,\mathrm{k\Omega}$. Finally, the low-pass filter consisted of a $R_F = (1.001 \pm 0.001)\,\mathrm{k\Omega}$ resistor and a $C_F = 10\,\mathrm{nF}$ capacitor.

The output V_{out} of the amplifier is inversely proportional to the resistance of the gold wire junction R_G, and the latter can thus be measured using the equation

$$R_G = R_A \left(\frac{R_{D2}}{R_{D1}}\right)\left(\frac{V_-}{V_{\mathrm{out}}}\right), \qquad (3)$$

where V_- is the negative rail voltage (here, $-10.00\,\mathrm{V}$). The reciprocal of Eq. 3 yields the conductance of the junction.

A junction conductance of $G \equiv 1/R_G = G_0$ should

produce an output signal of 168 mV. Therefore, to capture breaking traces, we set the falling slope trigger level to 120 mV and offset the trigger in time so that the majority of the trace buffer would be prior to the trigger event, hopefully containing several steps at integer multiples of the lowest voltage plateau.

By tapping the lab bench and carefully freezing the oscilloscope as stepped traces appeared, we could sketch the pattern of steps and measure their heights using the oscilloscope's cursor tools. Steps in the traces were sharply defined, indicating the breaking of individual transmission channels. However, the height of the lowest step was quite variable, and the higher plateaus were often not integer multiples of the lower ones. These traces confirm the potential viability of this simple method, but the variability in the results and the slow, manual process of obtaining them suggest that an automated setup capable of gathering large numbers of traces would do much to increase repeatability and precision.

In the second phase of our study, we substituted a piezoelectric actuator for the uncontrolled lab bench vibrations. One small gold wire attached to a fine copper lead was fixed to the actuator using double-sided cellophane tape. Another was fixed to a micrometer stage that could be brought closer to the actuator with a finely-pitched screw. A pocket knife with a right-angle screwdriver enabled us to position this stage quite precisely.

For the bulk of our collection runs, the actuator was driven by a triangle-wave signal with a peak-to-peak amplitude of 2.68 V and a DC offset of approximately -4.6 V. We ultimately settled on a driving frequency of 0.5 Hz, which provided the most reproducibility in forming and breaking contacts on an observable timescale. As the oscilloscope can only log data to the PC at a rate of approximately 1.4 Hz, we do not significantly compromise our data acquisition rate by choosing such a slow driver. Figure 2 illustrates the formation and breakage of contact between the two gold wires as the actuator is driven to close and open the microscopic gap separating them.

To assess the calibration of the oscilloscope and account for any voltage offsets present in the circuit, we independently calibrated the current-to-voltage amplifier by recording traces of its output while substituting a series of known resistances for R_G. Uncertainties in the resistances were derived from variability in the multimeter readings, while the standard deviation of the oscilloscope trace provided the uncertainty in the amplifier output. The measurements taken in this calibration process are collected in Table I.

Performing a weighted least squares-fit to the linear model

$$G = \alpha V_{\text{out}} + \beta \tag{4}$$

yields the calibration coefficients $\alpha = (498 \pm 4)\,\mu\text{S/V}$ and $\beta = (-0.596 \pm 0.089)\,\mu\text{S/V}$. The calibration points and their fit are plotted in Fig. 3. For comparison, taking the reciprocal of Eq. 3 leads to an expected value of $\alpha = (494 \pm 1)\,\mu\text{S/V}$, which is consistent with the results of this fit. The offset β, however, is inconsistent with zero, and this offset is not due to a miscalibration of the DSO.

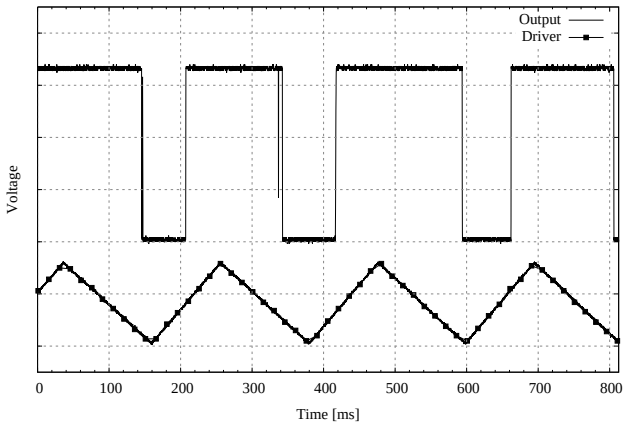

Figure 2 Oscilloscope trace illustrating breaking behavior synchronized with gold wire displacement. The upper trace corresponds to the output of the current-to-voltage amplifier, while the lower trace corresponds to the driving voltage for the piezoelectric transducer.

Table I Resistances and output voltages used to calibrate the conductance measurement system.

Resistance [kΩ]	Amplifier Output [mV]
∞	10.6 ± 2.8
78.5 ± 0.05	36.9 ± 5.9
22.58 ± 0.01	100.9 ± 2.8
14.30 ± 0.01	153.7 ± 2.7
1.908 ± 0.001	1079 ± 11.7
1.47 ± 0.005	1358 ± 13.7

Once the micrometer stage and driving signal had been tuned to consistently bring the wires in and out of contact, data collection proceeded much as in the first phase. We applied a negative offset to the output of the amplifier in order to take advantage of the entire range of the analog-to-digital converter (ADC) in the DSO. The vertical scale was sufficient for observing conductance plateaus as high as $5G_0$ while still providing roughly 2% precision for signals in the vicinity of $1G_0$. As before, the DSO was set to trigger on the falling slope, but this behavior was highly unreliable and produced numerous spurious traces.

As the driving frequency was lower than the PC's maximum logging rate, we acquired approximately 30 traces each minute. False triggers and stray events account for about half of these, so roughly a half-hour of continuous data collection was required in order to accumulate 500 good traces. During this time, the DC offset of the driving signal had to be lowered every few minutes to prevent the contact from sticking closed.

When histogramming traces gathered by the DSO, we assume that each of the bins is of equal width. How-

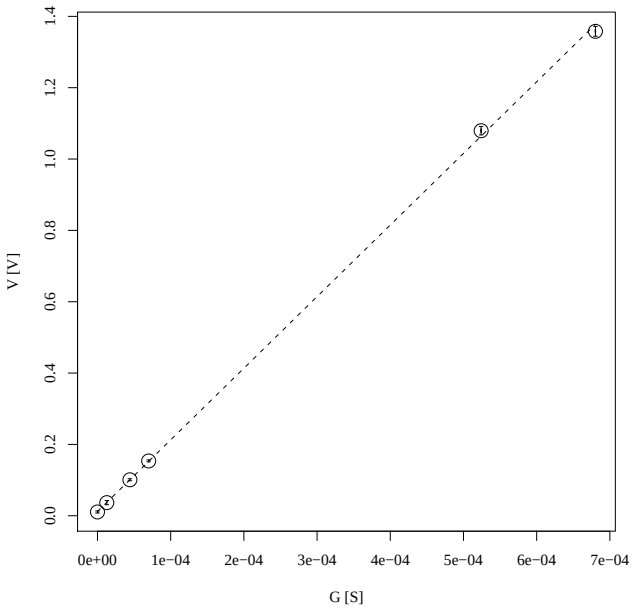

Figure 3 Calibration fit for the current-to-voltage amplifier powered by $\pm 10.00\,\mathrm{V}$ rails.

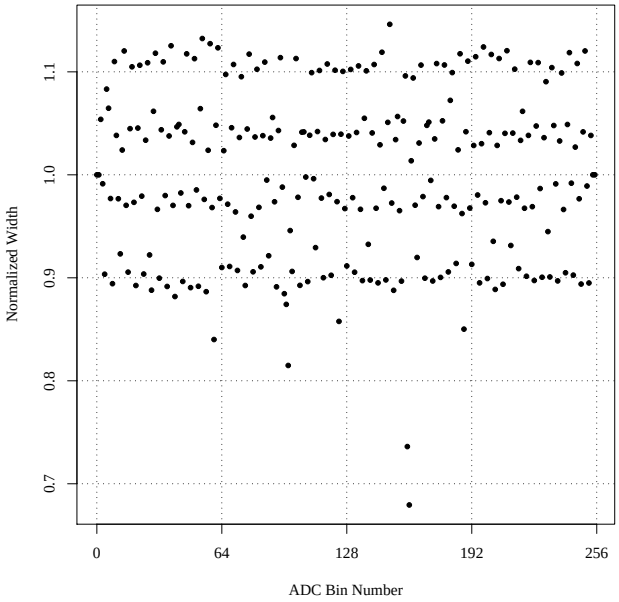

Figure 4 Differential nonlinearity of $\pm 10\%$ exposed via 8 million samples of a smoothly ramping voltage.

ever, ADCs are known to possess significant differential nonlinearities which manifest themselves in the form of nonuniform widths for each of the ADC bins. Failure to account for these nonlinearities introduces significant noise in the resulting histograms (Hansen *et al.*, 1997). Fortunately, these effective bin widths can be measured by histogramming traces of a smooth ramping voltage.

We generated a ramping voltage by viewing our triangle wave driver using the same oscilloscope settings as for collecting the output of the current-to-voltage amplifier. At this magnification, the waveform was seen as a monotonic voltage signal when triggered on either the ascending or descending slope. With the trigger centered in the collection buffer, the signal saturated the ADC at both early and late times, ensuring an even population of the intermediate channels. Figure 4 plots the number of counts recorded in each ADC channel for 257 ramping traces. These counts have been normalized about their mean in order to represent the relative widths of each channel.

The effective channel widths are divided into four distinct bands, the most extreme of which are 10% wider or narrower than the mean. The same analysis performed on the DSO's second input line showed similar behavior, but the extreme deviation bands were $> \pm 20\%$ off from the mean. Thus not all input lines on the DSO utilize ADCs of the same quality, and care must be taken when assigning input channels to minimize the noise in the most sensitive data.

By dividing the number of counts in each data histogram bin by the normalized height of that bin in the ramp histogram, we corrected our data for these nonlinearities, and the final histograms were noticeably smoother, as demonstrated in Fig. 5.

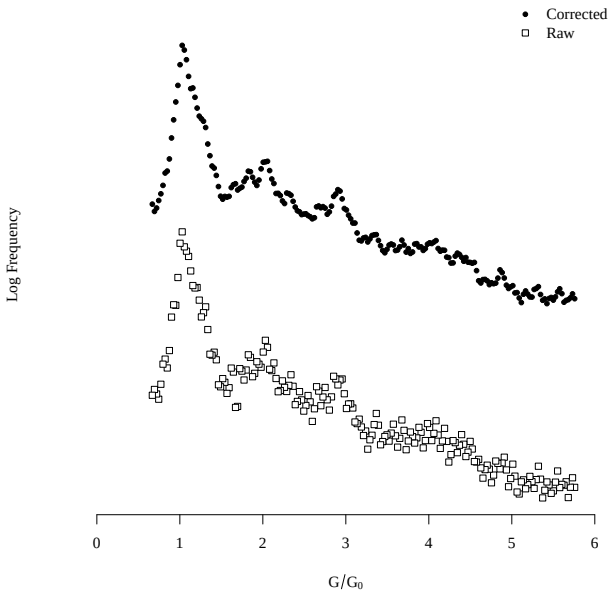

Figure 5 Comparison of raw and corrected histograms (logarithmic scale). Note the significant reduction in scatter for the corrected (top) curve.

IV. RESULTS

Our primary dataset consisted of 1037 raw traces, each containing 32 703 8-bit samples. In the DSO software's export format, this represents 1.1 GiB of on-disk data. However, the DSO software contains a bug causing the columns in these files to be offset in time with respect to one another by as many as 50 samples. This has no effect on our histogrammed results, but should be noted for future experiments using the same equipment. We analyzed this dataset using the GNU R software environment for statistical computing (R Development Core Team, 2008), while bulk data manipulation was accomplished using standard UNIX shell tools.

Traces captured by the DSO fell into several general categories. The oscilloscope's trigger is very sensitive to noise, so approximately half of the collected traces display an ascending slope (formation of contact instead of breaking) or consist of a relatively constant voltage at approximately the trigger level. Other traces accurately capture a breaking event, but the break is effectively instantaneous and does not form small numbers of nanowires. Visually, these contain a sharp exponential dropoff characterized by the low-pass filter. Finally, the remaining traces consist of a stepped voltage descent, indicative of quantized conductance.

For a preliminary dataset containing a relatively small number of traces, those of the first two varieties were eliminated by eye. The remaining traces were all included in subsequent analyses, regardless of whether or not the plateaus appear to correspond to integer multiples of G_0. An example of a particularly clear trace is plotted in Fig. 6. This trace has been smoothed for presentation using a Savitzky-Golay filter of length 501 (Press *et al.*, 2007), which visually clarifies the quantized behavior by removing noise and digitization artifacts. All quantitative analysis, however, was performed on the original, unsmoothed data.

Quality traces like that shown in Fig. 6 facilitate direct measurement of G_0 by computing the mean and standard deviation of the final plateau. Averaging the results of this procedure applied to seven exemplary traces, recorded in Table II, produced an estimate for the fundamental conductance of $G_0 = (81 \pm 11)\,\mu\text{S}$. When compared to the theoretical value of 77.5 μS, this is accurate to within 5%. With the relative uncertainty at 13%, these measurements are in statistical agreement with theory, but they are also not particularly constraining.

These traces also contained shorter-lived plateaus at non-integer multiples of G_0, including several well below this value. In terms of the Landauer formula (Eq. 1), these indicate that some modes have a transmission probability of $< 100\%$. This can be caused by impurities due to contamination of the open-air junction, and such impurities in more controlled experiments have indeed yielded conductance plateaus in the range of 0.1 to 0.2 G_0 (Rodrigues *et al.*, 2000).

For datasets containing larger numbers of traces, as are necessary to construct statistically significant histograms, manual sifting as described above is not practical. We instead developed a sieve algorithm to reject traces whose average slope is larger than some cutoff. This eliminated flatline traces as well as spurious triggers on ascending slopes. When applied to our collection of 1037 traces, this algorithm selected 634 for further analysis.

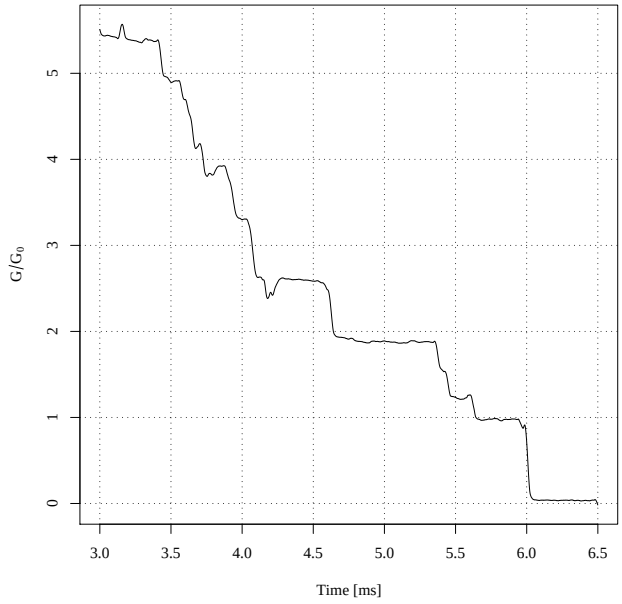

Figure 6 Smoothed, high-quality trace of conductance during breaking (in units of the fundamental conductance) showing clear evidence of quantization.

Table II Mean values of plateaus near G_0 for seven high-quality traces showing strong evidence of quantization.

Mean Conductance [10^{-5} S]	Standard Deviation [10^{-5} S]
7.88	0.35
7.46	0.47
7.26	0.45
7.90	0.28
8.18	0.48
10.48	0.36
7.57	0.30

The voltage readings for each selected trace were collected into a histogram using the 256 bins naturally provided by the 8-bit digitization process. After summing the histograms for all of the traces, these voltage bins were converted to conductance bins using the calibration fit described by Eq. 4. After adjusting the counts to compensate for the nonuniform ADC bin widths, we obtained the histogram shown in Fig. 7.

The first histogram peak corresponds to $G/G_0 = 1.003 \pm 0.019$, where the uncertainty in its voltage location is taken to be half of the bin width ($\sigma_V = 2\,\text{mV}$). This uncertainty is combined with that associated with the

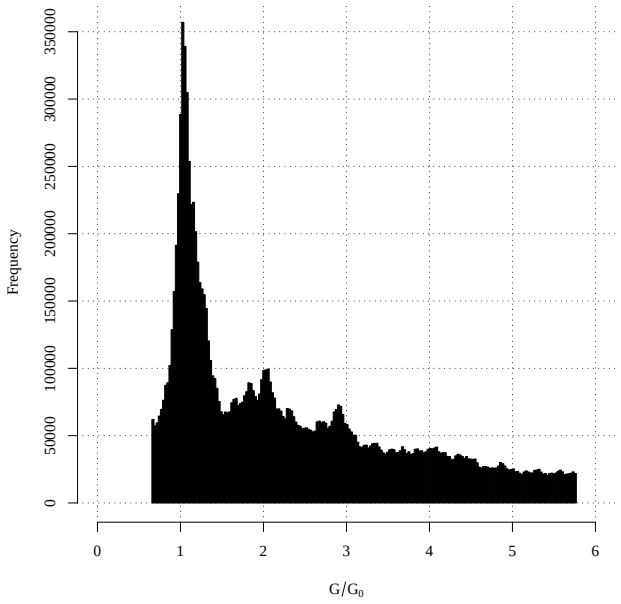

Figure 7 Corrected histogram of conductance (in units of the fundamental conductance) for a collection of 634 automatically-selected breaking traces. Extreme values (corresponding to open and closed circuits) have been omitted for clarity.

calibration fit to compute our final error bars as

$$\sigma_G{}^2 = (V\sigma_\alpha)^2 + (\alpha\sigma_V)^2 + \sigma_\beta{}^2 \,. \tag{5}$$

The contribution to the overall uncertainty due to ambiguity in the peak bin location is of the same magnitude as the error induced by the calibration fit, indicating that the precisions of our measurements were well-matched. Switching to a 12-bit DSO, for example, would not improve our result without a comparable increase in the quality of our calibration. Given these uncertainties, our measurement of G_0 is precise to 2% and happens to agree with the theoretical value to within 0.3%. This accuracy is quite impressive, as 1% deviations from this value are expected in far more controlled experiments using 2D electron gas heterojunctions (van Houten and Beenakker, 1996).

If a statistical distribution is symmetric about a maximum, then the mean of data points surrounding that maximum provides an estimate of its location. By taking weighted averages of voltages surrounding the peak, the estimated peak center shifts to as high as $G/G_0 = 1.010$. However, the histogram's peak does not appear to be symmetric even away from the center, casting doubt on the validity of this procedure. As these results are consistent with our more conservative estimate using only the single largest bin, and as that bin is significantly taller than its closest neighbors, we choose not to alter our estimate for the value of G. However, this technique proves valuable when estimating the center of wider peaks without fitting to an assumed peak shape.

The second peak consists of three nearly-equal histogram bars centered around bin #147. Averaging over a cluster of 5 bars of heights greater than 85 000 counts and using the full bin width of 4 mV as the uncertainty yields an estimate of $(2G)/G_0 = 2.005 \pm 0.033$, which is quite consistent with the expected value of 2. Even better is the value $(2G)/G = 2.000 \pm 0.050$, showing that the second peak is almost exactly equal to twice the conductance of the first measured peak.

Performing a similar analysis with the third peak, however, yields a value of $(3G)/G_0 = 2.879 \pm 0.037$, which is not consistent with being three times the fundamental conductance (and at $(3G)/G = 2.871$ is even less consistent with being equal to three times the first measured peak).

Previous studies have justified the addition of a constant resistance of a few hundred Ohms to each conductance measurement. This procedure stretches the histogram peaks to the right and has been necessary to line up higher peaks with integer multiples of the first (Hansen *et al.*, 1997). Among the proposed sources for this resistance are the resistances of the copper leads and the effective gold leads attached to the nanowires. While applying this procedure here might move the third peak closer to $3G_0$, it would likely reduce the accuracy of the first and second peak. Since no more than three peaks are visible in our data, we currently have insufficient information for fitting or evaluating such a resistance.

V. CONCLUSION

We have successfully demonstrated that one can observe the quantization of conductance in gold nanowires using a tabletop apparatus at room temperature. Furthermore, the resulting conductance histogram clearly shows three peaks near integer multiples of the theorized fundamental unit of conductance. These peaks can be determined with an uncertainty of less than 4%, and two of the three are in excellent statistical agreement with their predicted locations.

These procedures can be straightforwardly extended to pursue further investigation in several directions. By zooming the DSO in on the known location of the lowest plateau, we could measure the value of G_0 with even greater precision. This would also require a more precise calibration, possible by using a greater number of known reference resistors in the range of 13 kΩ.

Alternately, by zooming the oscilloscope out in both voltage and time, we could capture plateaus at multiples of the fundamental conductance beyond the third. Triggering the DSO at a much higher voltage allowed Costa-Krämer et al. to observe conductance plateaus at as high as $40G_0$ (Costa-Krämer *et al.*, 1995). With a greater number of traces, higher peaks should become more apparent in the histogram. Unevenness in the spacing of these peaks could perhaps even be used as a measure of the contamination of the contact. Additionally, the areas

under these peaks could potentially be used to estimate relative nanowire lifetimes.

Finally, once the locations of the first conductance peaks have been established, the sieve algorithm could be expanded to classify traces into several groups (depending on whether or not the first or second plateaus are present, for instance). The relative populations of these groups could then be used to confirm the relative frequencies of different nanowire atomic configurations as reported by Rodrigues et al. (Rodrigues *et al.*, 2000).

Acknowledgments

I would like to express my gratitude to Dr. Paul McEuen for giving me the opportunity to freely develop this experiment as well as for many fruitful suggestions when I failed to reproduce consistent results. I would also like to thank Mr. Nicholas Szabo, Jr. for rapidly replacing a transistor in my broken power supply and for providing me with the digital oscilloscope and software that allowed this study to significantly improve on the precision of previous efforts.

References

Costa-Krämer, J. L., N. García, P. García-Mochales, and P. A. Serena, 1995, Surface Science **342**(1-3), L1144 , ISSN 0039-6028.

Hansen, K., E. Lægsgaard, I. Stensgaard, and F. Besenbacher, 1997, Phys. Rev. B **56**(4), 2208.

van Houten, H., and C. Beenakker, 1996, Physics Today **49**(7), 22, URL `http://link.aip.org/link/?PTO/49/22/1`.

Khurana, A., 1988, Physics Today **41**(11), 21, URL `http://link.aip.org/link/?PTO/41/21/1`.

Press, W. H., S. A. Teukolsky, W. T. Vetterling, and B. P. Flannery, 2007, *Numerical Recipes 3rd Edition: The Art of Scientific Computing* (Cambridge University Press, New York, NY, USA), ISBN 0521880688, 9780521880688.

R Development Core Team, 2008, *R: A Language and Environment for Statistical Computing*, R Foundation for Statistical Computing, Vienna, Austria, ISBN 3-900051-07-0, URL `http://www.R-project.org`.

Rodrigues, V., T. Fuhrer, and D. Ugarte, 2000, Phys. Rev. Lett. **85**(19), 4124.